Acta Oceanol. Sin., 2015, Vol. 34, No. 9, P. 78–84
DOI: 10.1007/s13131-015-0700-1
http://www.hyxb.org.cn
E-mail: hyxbe@263.net

Projection of the Zhujiang (Pearl) River Delta's potential submerged area due to sea level rise during the 21st century based on CMIP5 simulations

XIA Jiangjiang[1*], YAN Zhongwei[1], ZHOU Wen[2], FONG Soi Kun[3], LEONG Ka Cheng[3], TANG Iu Man[3], CHANG S W[3], LEONG W K[3], JIN Shaofei[1]

[1] Key Laboratory of Regional Climate-Environment for Temperate East Asia, Institute of Atmospheric Physics, Chinese Academy of Sciences, Beijing 100029, China

[2] Guy Carpenter Asia-Pacific Climate Impact Centre, School of Energy and Environment, City University of Hong Kong, Hong Kong, China

[3] Macao Meteorological and Geophysical Bureau, Macao, China

Received 26 September 2014; accepted 23 March 2015

Abstract

Projections of potential submerged area due to sea level rise are helpful for improving understanding of the influence of ongoing global warming on coastal areas. The Ensemble Empirical Mode Decomposition method is used to adaptively decompose the sea level time series in order to extract the secular trend component. Then the linear relationship between the global mean sea level (GMSL) change and the Zhujiang (Pearl) River Delta (PRD) sea level change is calculated: an increase of 1.0 m in the GMSL corresponds to a 1.3 m (uncertainty interval from 1.25 to 1.46 m) increase in the PRD. Based on this relationship and the GMSL rise projected by the Coupled Model Intercomparison Project Phase 5 under three greenhouse gas emission scenarios (representative concentration pathways, or RCPs, from low to high emission scenarios RCP2.6, RCP4.5, and RCP8.5), the PRD sea level is calculated and projected for the period 2006–2100. By around the year 2050, the PRD sea level will rise 0.29 (0.21 to 0.40) m under RCP2.6, 0.31 (0.22 to 0.42) m under RCP4.5, and 0.34 (0.25 to 0.46) m under RCP8.5, respectively. By 2100, it will rise 0.59 (0.36 to 0.88) m, 0.71 (0.47 to 1.02) m, and 1.0 (0.68 to 1.41) m, respectively. In addition, considering the extreme value of relative sea level due to land subsidence (i.e., 0.20 m) and that obtained from intermonthly variability (i.e., 0.33 m), the PRD sea level will rise 1.94 m by the year 2100 under the RCP8.5 scenario with the upper uncertainty level (i.e., 1.41 m). Accordingly, the potential submerged area is 8.57×10^3 km^2 for the PRD, about 1.3 times its present area.

Key words: sea level, Zhujiang (Pearl) River Delta (PRD), representative concentration pathways (RCPs), CMIP5, submerged area, Ensemble Empirical Mode Decomposition (EEMD)

Citation: Xia Jiangjiang, Yan Zhongwei, Zhou Wen, Fong Soi Kun, Leong Ka Cheng, Tang Iu Man, Chang S W, Leong W K, Jin Shaofei. 2015. Projection of the Zhujiang (Pearl) River Delta's potential submerged area due to sea level rise during the 21st century based on CMIP5 simulations. Acta Oceanologica Sinica, 34(9): 78–84, doi: 10.1007/s13131-015-0700-1

1 Introduction

Under the background of global warming, sea level rise could directly impact land area, population, and economic activity in coastal regions (Anthoff et al., 2006; IPCC, 2007a). More frequent occurrences of land loss, flooding, storm surges, and hurricanes will be a consequence of sea level rise (Sweet et al., 2013), and the damage resulting from such events will not only obstruct sustainable economic/ecological development but will also threaten the lives of millions. Therefore, projecting sea level change is beneficial for mitigating and adapting to the potential damage caused by climate change.

Sea level change includes both absolute and relative change. Absolute sea level (geocentric sea level) is measured with respect to a geocentric reference, e.g., the reference ellipsoid, and can be obtained from satellite altimetry. Relative sea level is measured using tide gauges and considers extra coastal impacts such as land subsidence at a given location. Church et al. (2013) reported that the global mean sea level (GMSL) rose during the period 1901–2010 at a rate of about 1.7 mm per year as evidenced by tide gauges, and for the period 1993–2010 at a rate of about 3.2 mm per year as evidenced by satellite altimetry. The China Sea has experienced a rise of about 2.6 mm per year for the last three decades (tide gauges) according to the 2010 China Sea Level Communique, and 4.99 mm per year from 1993 to 2011 (satellite altimetry; Wang, 2013). It is clear that the rate of sea level rise for the China Sea is larger than that of the GMSL.

It has been documented that the rise in GMSL in the 20th century is due mainly to ocean thermal expansion and glacier melting caused by anthropogenic global warming, which is almost certain to continue in the future (IPCC, 2013; Li et al., 2013). Thus it is beneficial to investigate sea level rise during the 21st century under this scenario. In fact, plenty of studies have projec-

Foundation item: The Strategic Priority Research Program of the Chinese Academy of Sciences No. XDA11010404; the National Natural Science Foundation of China under contract Nos 41375096, 41175079 and 41405082; the Macao Meteorological and Geophysical Bureau Project under contract No. 9231048.
*Corresponding author, E-mail: xjj_8448@163.com

ted China's sea level change for the 21st century based on the output from coupled ocean-atmosphere general circulation models (CGCMs) under global warming scenarios (Shi et al., 2000; Huang et al., 2001; Liu, 2004; Li et al., 2009; Li et al., 2011; Zuo et al., 2013). For example, by considering the projected GMSL rise based on results from CGCMs and local land subsidence, Shi et al. (2000) suggested a 0.25 to 0.5 m relative sea level rise for the Changjiang (Yangtze) River Delta by the year 2050. Li et al. (2011) reported a sea level rise of 0.28 to 0.64 m in China by the end of the 21st century.

The latest projections of the rise in GMSL under different greenhouse gas (GHG) emission scenarios, simulated by 21 Coupled Model Intercomparison Project Phase 5 (CMIP5) CGCMs (Church et al., 2013), are consistent with the "representative concentration pathways (RCPs)" (Moss et al., 2010). The RCP scenarios include a range of specified concentrations, as described in the IPCC's Fifth Assessment Report (IPCC, 2013). Projections of GMSL rise for each RCP scenario are based on changes in thermal expansion, glaciers, the Greenland ice sheet, the Antarctic ice sheet, and land water storage. Since the Fourth Assessment Report (AR4) (IPCC, 2007b), confidence in the projections of GMSL rise has increased because of the improved physical understanding of the components of sea level, the improved agreement of process-based models with observations, and the inclusion of ice-sheet dynamical changes. The projections of GMSL under RCP scenarios are larger than in AR4, primarily because of improved modeling of land-ice contributions. However, the rates of regional sea level change can differ from GMSL and have yet to be analyzed.

Although these latest simulations have contributed to a general knowledge of sea level changes on a global scale (Church et al., 2013), local sea level rise is still not well studied, e.g., the coast of the Zhujiang (Pearl) River Delta (PRD) in China. The PRD is a highly developed region, which at the end of 2012 was occupied by 56.90 million people (4.2% of national population) and gross domestic product (GDP) of 757.5 billion US$ (9.2% of national GDP; Chan et al., 2013). It is close to the two special Chinese administrative regions of Hong Kong (7.18 million people, 263.3 billion US$) and Macau (0.58 million people, 43.6 billion US$). The PRD combined with Hong Kong and Macau (called the Greater PRD) will continue to be an economic hotspot in China. The PRD has very low altitudes, which is likely to suffer from sea level rise in the future (Li et al., 1993). Thus, in this study we aim to investigate the relative sea level change during the 21st century for the PRD under the latest greenhouse gas (GHG) emission scenarios provided by CMIP5, and to calculate the potential submerged area for the PRD.

2 Data

2.1 *Satellite altimeter data*

In this study we use the combined TOPEX/Poseidon, Jason-1 and Jason-2/OSTM geocentric sea level fields for the period 1993–2012, developed by Church and White (2011), on a 1°×1° grid. We use the version with the inverse barometer correction and the glacial isostatic adjustment. The dataset, with 19 valid grids covering the target region (19.5°–22.5°N, 110.5°–117.5°E, Fig. 1) of this study, can be accessed from: http://www.cmar.csiro.au/sealevel/sl_data_cmar.html (accessed June 5, 2014).

In addition, the time series of GMSL calculated using this dataset is also available from the website above.

2.2 *In situ sea level data*

Monthly sea-level data from four tide gauge stations near the Zhujiang (Pearl) River Delta (Table 1) were downloaded from the Permanent Service for Mean Sea Level (Holgate et al., 2013; PSMSL, 2014) website (http://www.psmsl.org). The period of 1993–2012 is chosen. A time series of GMSL calculated using global tide gauges is available from: http://www.cmar.csiro.au/sealevel/sl_data_cmar.html (accessed June 5, 2014). It is worth noting that relative sea level change observed at tide gauge stations could include a part influenced by the land subsidence (Ren and Zhang, 1993; Huang et al., 2001), which is considered as the long-term change.

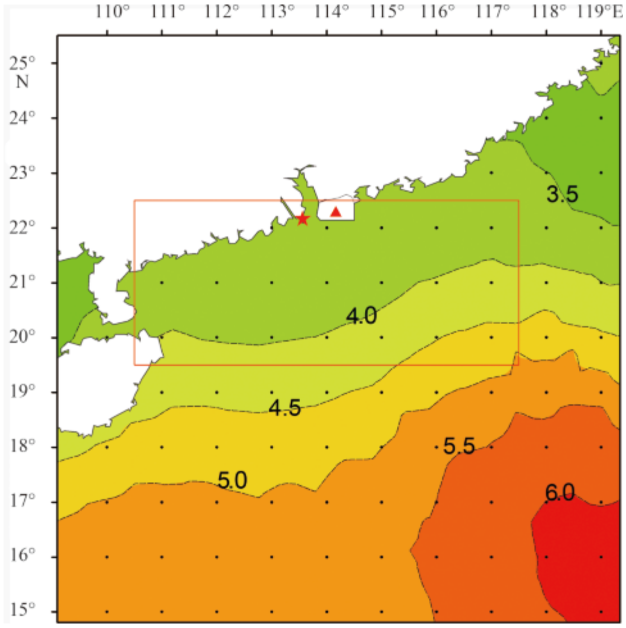

Fig. 1. Map of the rates of change in geocentric sea level for the period 1993–2012 from satellite altimetry (values are given near the contour lines). Unit: mm/a. The star and triangle identify Macau and Hong Kong, respectively.

Table 1. Data from the four tide gauge stations.

Station name	PSMSL ID	North latitude	East longitude	Province or region
Zhapo	933	21.583°	111.817°	Guangdong
Tai Po Kau, Tolo Harbour	1034	22.443°	114.184°	Hong Kong
Tsim Bei Tsui	1366	22.487°	114.014°	Hong Kong
Quarry Bay	1674	22.291°	114.213°	Hong Kong

2.3 *Projected global sea level change*

Simulations by global coupled ocean-atmosphere general circulation models (CGCMs) provide the primary basis for studying possible future climate change (Kharin et al., 2007). The CMIP5 projections are forced by GHG emission scenarios consistent with the RCPs. GMSL rise values for the period 2006–2100 under the RCP2.6, RCP4.5, and RCP8.5 scenarios (Table 2) are used in this study. The radiative forcing in RCP8.5 increases throughout the 21st century and reaches a level of about 8.5 W/m^2 by the year 2100. In addition to this "high" RCP8.5 scenario, the intermediate RCP4.5 scenario reaches a level of about 4.5 W/m^2 by 2100. The RCP2.6 scenario is described as a peak-and-decay low scenario, in which the radiative forcing will reach a maximum near the middle of the 21st century before decreasing to an eventual low of 2.6 W/m^2 (Taylor et al., 2012). A dataset of GMSL rise values from a collection of 21 CGCMs (see the Supplementary Material of Church et al. (2013) for more details) for the period 2006–2100 is used, including the median and likely range.

Table 2. Desirable types of representative concentration pathways

Name	Shape of pathway	Radiative forcing	Equivalent concentration ppm
RCP8.5	continued rise	8.5 W/m^2 at stabilization in 2100	about 1 370 CO_2–eq
RCP4.5	stabilization without exceeding target level	4.5 W/m^2 at stabilization in 2100	about 650 CO_2–eq
RCP2.6	peak and decline stabilization	less than 3 W/m^2 in 2100	about 490 CO_2–eq

2.4 *Digital elevation model (DEM)*

The DEM of the Zhujiang (Pearl) River Delta has a spatial resolution of 3″, which is about 90 m. The DEM is based on the data collected by the 2000 Shuttle Radar Topography Mission. The area 21°–24°N, 112°–115°E is chosen as the target. The data used in this study are available from:http://www.viewfinderpanoramas.org/dem3.html (accessed 30 April, 2014).

The mean sea surface height above geoid over the period 1993–1999 is calculated by the MDT_CNES-CLS09 model, which is computed from satellite altimetry data from the satellite mission OSTM/Jason-2. The data are available from:http://www.aviso.altimetry.fr/en/home.html (accessed 24 June, 2014).

Both the DEM and the mean sea surface height are in meters referenced to the WGS84/EGM96 geoid (NASA, 1998). Therefore, changes in the area that is below mean sea level can be calculated. The present sea level is 1.04 m in the PRD.

3 Method

The GMSL obtained from both the satellite altimeter and the gauge stations shows a nearly linear trend during 1993–2012 (Church et al., 2013), as shown in Fig. 2a. Regional sea level change could differ substantially from the GMSL, due to regional differences in heating and circulation changes (Wu et al., 2007; Hamlington et al., 2014; IPCC, 2013). Therefore, in this study, for each grid and for each tide gauge station, the secular change component (nearly linear trend, Fig. 2b) is extracted from the raw sea level time series using the Ensemble Empirical Mode Decomposition (EEMD) method, which was developed for nonlinear and nonstationary time-series analysis (Huang et al., 1998; Huang and Wu, 2008; Wu and Huang, 2009). The secular change is defined as the last component of EEMD output. The secular change in the global mean surface air temperature, extracted using EEMD, is considered to be the consequence of the buildup of well-mixed greenhouse gases (Wu et al., 2011). Evidence is emerging that other components, e.g., the multidecadal variability component, extracted using the EEMD from various data could also reflect the physical processes (Xia et al., 2013; Gao et al., 2015; Qian and Zhou, 2014). Ocean thermal expansion and glacier melting have been the dominant contributors to the nearly linear rise of the GMSL in the 20th century (Church et al., 2013). We believe that the nearly linear secular change obtained from the local sea level time series is probably dominated by ocean thermal expansion and glacier melting. Therefore, we should be able to establish a linear relationship between the changes in local

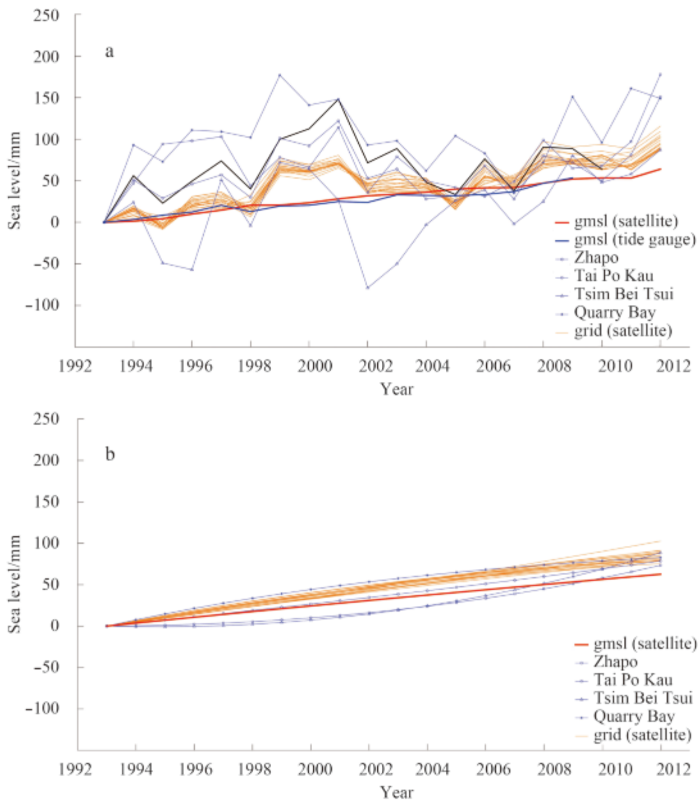

Fig. 2. Changes in geocentric sea level, from satellite altimetry and selected tide gauge stations, for the period 1993–2012 with respect to the year 1993. a. Raw time series, and b. secular changes obtained by using EEMD. The thick blue curve indicates the GMSL obtained using global tide gauges, while the thick red curve indicates the GMSL obtained using the satellite altimeter.

sea level and GMSL. The regression coefficients of the secular change components onto the GMSL are calculated, as shown in Fig. 3. As we mentioned in Section 2.2, the long-term change of relative sea level change at tide gauge stations could be influenced by the land subsidence. That is the reason that the regression coefficients are calculated only for grids. Using this linear relationship and the projected GMSL under the RCPs in the 21st century, we can reconstruct the geocentric sea level rise in the Zhujiang (Pearl) River Delta.

4 Results

4.1 *Projected absolute sea level rise in the PRD*

Figure 3a shows the linear trends of the secular change component for each grid or gauge station, as well as the GMSL. Between 1993 and 2012, the GMSL rose 3.28 mm/a. The rate of sea level rise near the PRD, for the grids, was higher than that of GMSL, ranging from 4.1 mm/a to 4.8 mm/a (uncertainty intervals 5%–95%). The median value is 4.4 mm/a. The regression coefficients of the secular change components onto the GMSL are shown in Fig. 3b. This suggests that for every 1 mm/a rise in GMSL, there should be a larger rise (1.3 (1.25 to 1.46) mm/a) in sea level near the Zhujiang (Pearl) River Delta.

Simulated by CMIP5 CGCMs, there is high confidence in projections of thermal expansion and Greenland surface mass balance, and medium confidence in projections of glacier mass loss and Antarctic surface mass balance. Compared to 1986–2005, for the period 2081–2100, GMSL rise is likely to be in the 5% to 95% range of projections, which give 0.26 to 0.55 m for RCP2.6, 0.32 to 0.63 m for RCP4.5, and 0.45 to 0.82 m for RCP8.5 (Church et al., 2013). Then, using the linear relationship and the projected GMSL rise under these RCPs, the local sea level rise is reconstructed (Fig. 4).

Figure 4 shows that by the year 2050, RCP2.6 gives the least amount of PRD sea level rise (0.29 (0.21 to 0.40) m) (median, (likely range)) and RCP8.5 gives the most (0.34 (0.25 to 0.46) m). RCP4.5 has a rise of 0.31 (0.22 to 0.42) m by the late 21st century. This indicates that the median projection for PRD sea level in all three RCP scenarios lies within a range of 0.2 m until the middle of the century. However, by 2100, they have a larger spread of more than 0.5 m. The likely ranges are 0.59 (0.36 to 0.88) m for RCP2.6, 0.71 (0.47 to 1.02) m for RCP4.5, and 1.0 (0.68 to 1.41) m for RCP 8.5.

4.2 *Relative sea level rise in the PRD due to subsidence*

Because relative sea level change can be considerably influenced by coastal impacts, for example, the land subsidence (Ren

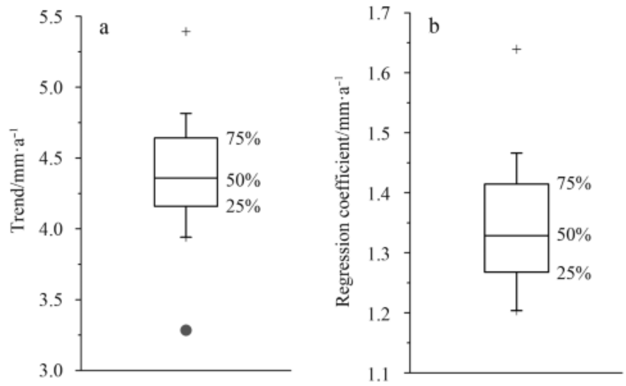

Fig. 3. Distribution of trends of sea level rise for the period 1993–2012 (the trend is calculated using the secular change component of sea level for each grid) (a) and regression coefficients of the secular change components onto the GMSL (the box-and-whiskers distribution is calculated using the satellite altimeter from the 19 grids) (b). The bottom and top of the box are the 25th and 75th percentiles, respectively, and the band near the middle of the box is always the 50th percentile. The black bands are within 1.5 interquartile range of the lower/upper quartile, and + is the extreme value. The gray circle indicates the GMSL.

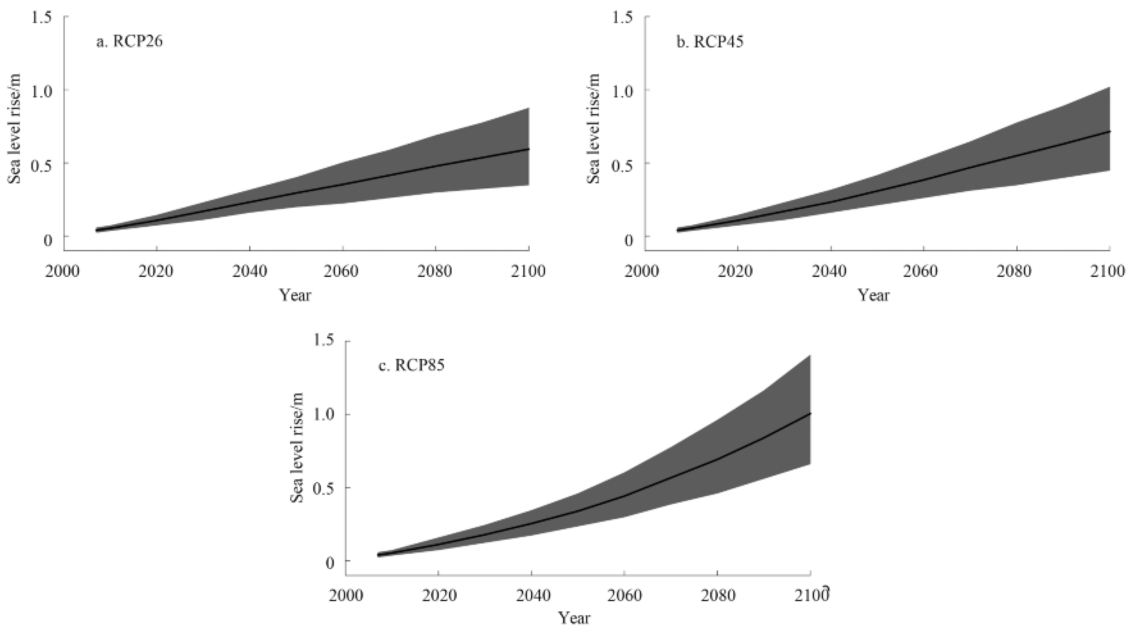

Fig. 4. Projected PRD sea level rise for the period 2006–2100 relative to 1986–2005 for the RCP2.5 (a), RCP4.5 (b), and RCP8.5 (c) scenarios, respectively. Gray shaded bands show the 5% to 95% uncertainty range for these simulations from 21 climate models.

and Zhang, 1993; Huang et al., 2001). Thus it should be considered when projecting relative PRD sea level rise and its impacts in China. In this study, the land subsidence rate in the PRD is estimated using empirical values. Huang et al. (2001) estimated the rate of land subsidence for the period 1951–1989 by analyzing the leveling data from 132 stations along the coastal PRD. They suggested a land subsidence rate of about 1.5–2.0 mm per year. If the future land subsidence rate remains the same as the past, the amplitude of the relative sea level rise by the years 2050 and 2100 is calculated to be about 0.075–0.10 m and 0.15–0.20 m, respectively.

4.3 *Extreme values from intermonthly variability*

Previous studies (e.g., Gu and Li, 2009; Wang et al., 2014) found that high frequency fluctuations (such as interannual and intermonthly variability) of sea level in China are affected by the El Niño Southern Oscillation. In this study, the sea level rise is projected based on the relationship calculated using the secular change (Fig. 2b), which is extracted by applying EEMD. In this way, the high frequency fluctuations are removed. However, it is worth noting that the extreme values from high frequency fluctuations are quite large (Fig. 2a), which could not be ignored while analyzing the effects of projected sea level rise for the 21st century.

In this study, the intermonthly variability is defined as the sum of all the components, except the secular change component, from the original monthly sea level time series for each tide gauge station or grid. It follows the generalized extreme value (GEV) probability density function (Fig. 5), by applying the Kolmogorov-Smirnov Test (Massey, 1951) to the intermonthly variability. Consequently, the observed maximum of the intermonthly variability is 0.33 m, corresponding to a return period of about 200 years.

4.4 *Potential submerged area under theextreme conditions*

In this study, three items are considered when estimating potential submerged area: absolute sea level rise under the different RCPs, relative sea level rise due to subsidence, and extreme values from intermonthly variability. We focus in particular on the results under the extreme conditions by the year 2100: the upper uncertainty level under the RCP8.5 scenario (i.e., 1.41 m), the extreme value of relative sea level due to land subsidence (i.e., 0.20 m), and the extreme value obtained from intermonthly variability (i.e., 0.33 m). Considering all three items, the sea level will rise 1.94 m by the year 2100 under RCP8.5. Then the worst situation will be 1.94 m of sea level rise for the PRD by the end of the 21st century. As the present sea level is 1.04 m, the projected maximum sea level will be 2.98 m.

With this projection, we can evaluate the area that is below sea level near the Zhujiang (Pearl) River Delta. As the DEM has a vertical resolution of 1 m, we can only evaluate the area below sea level with every PRD sea level rise of 1 m. Then the 3rd degree polynomial is used to fit the discrete values of the time series of the area below sea level (Fig. 6). The present PRD sea level is 1.04 m, while the area below PRDSL is about 6.46×10^3 km^2 (Fig. 7a). When the PRD sea level is 2.98 m, the area below sea level will be 8.57×10^3 km^2 (Fig. 7b), about 1.3 times the present area under sea level.

Church et al. (2013) declared that sustained global warming over a certain threshold (more than 2°C but less than 4°C) above preindustrial levels would lead to the near-complete loss of the Greenland ice sheet over a millennium or more, causing a GMSL rise of about 7 m. According to this and the relationship we obtained between PRD sea level and GMSL (Fig. 3b), the PRD sea level could rise about 10 m in this extreme situation.

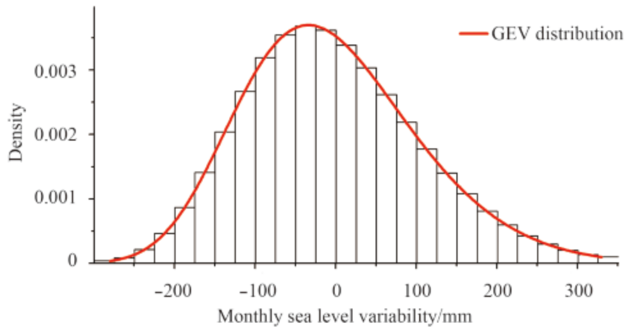

Fig. 5. GEV probability density of intermonthly sea level variability, at the 1% significance level. The shape parameter k is −0.141 1, the scale parameter sigma is 100.533 4, and the location parameter mu is −48.706 2.

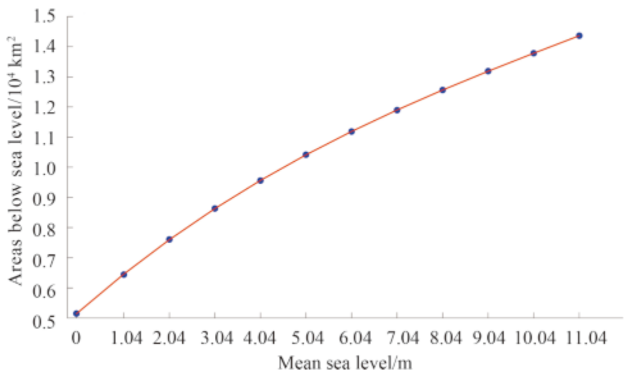

Fig. 6. Area below sea level with various magnitudes of sea level rise. The 1.04 m is the present mean sea level. The 2.98 m could be considered the worst possible situation of projected sea level rise under the RCP8.5 scenario. The 3rd degree polynomial is $A=1.95\times S^3-66.51\times S^2+1\,331.25\times S+5\,142.19$, where A indicates the area below sea level, and S indicates the PRD sea level.

5 Discussion

In this study, the projected PRD potential submerged area due to sea level rise for the 21st century is based on a series of ideal scenarios, (1) the RCP scenarios, a range of specified GHG emission scenarios, (2) the rates of land subsidence in PRD remain the same, (3) the probability density function of intermonthly variability remains the same for the 21st century. Thus there is large uncertainty in estimating the sea level rise in PRD for the 21st century. For example, the secular change of sea level may influenced by low-frequency natural climate variability such as Pacific Decadal Oscillation (Gu and Li, 2009; Hamlington et al., 2014). Besides, some other factors could also change the land subsidence rate. For example, the earthquake with magnitude of 6.1 in Gang Dong province made a sudden relative sea level drop in Macau in 1962 (Yim, 1989). The intermonthly variability may also not follow the same GEV probability density function at the century scale. A full discussion of all these uncertainties deserves a further study.

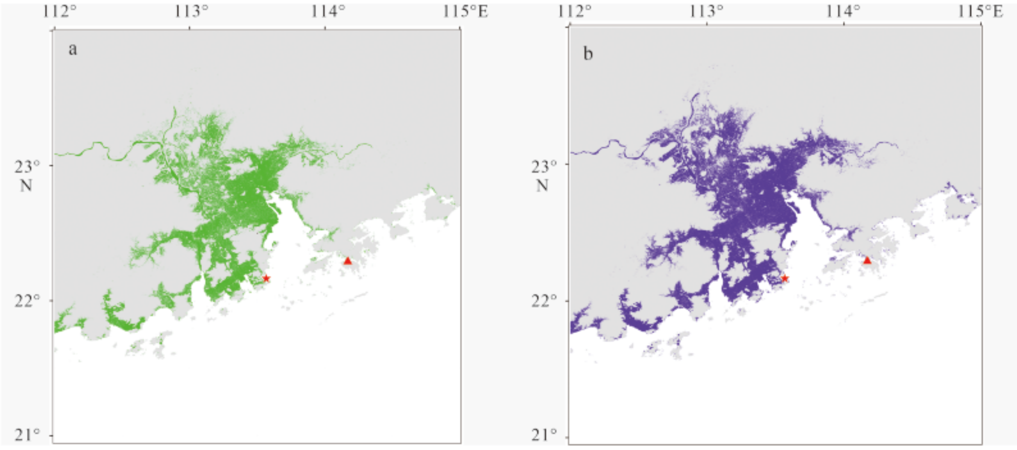

Fig. 7. Maps of the area below sea level with different amounts of sea level rise. The land DEM area below the present average sea level of 1.04 m over the period 1993–1999 (a), the sea level of 2.98 m (b) (1.94 m higher than the present sea level of 1.04 m). The star and triangle identify Macau and Hong Kong, respectively.

In addition, our results show the sea level rise based on monthly data from observations and models; however, a larger daily fluctuation of sea surface height than what is seen in monthly data could cause greater damage to coastal infrastructures and property. For example, tides, waves, storms, and typhoons could be enhanced due to sea level rise (Du and Zhang, 2000; Sweet et al., 2013). According to our results, the rate of sea level rise in the PRD is larger than the global rate, which could mean the PRD is likely to confront greater challenges in the future.

References

Anthoff D, Nicholls R J, Tol R S J, et al. 2006. Global and regional exposure to large rises in sea-level: A sensitivity analysis. This work was prepared for the Stern Review on the Economics of Climate Change. Tyndall Centre Working Paper 96

Chan T M H, Yung J H W, Chung M K. 2014. The greater Pearl River Delta. A report commissioned by Invest Hong Kong, 78

Church J A, Clark P U, Cazenave A, et al. 2013. Sea level change. In: IPCC. Climate Change 2013: The Physical Science Basis. Working Group I Contribution to the Fifth Assessment Report of the Intergovernmental Panel on Climate Change. Cambridge: Cambridge University Press

Church J A, White N J. 2011. Sea-level rise from the late 19th to the early 21st century. Surveys in Geophysics, 32 (4–5): 585–602

Du Bilan, Zhang Jinwen. 2000. Adaptation strategy for sea level rise in vulnerable areas along China's coast. Acta Oceanologica Sinica, 19(4): 1–16

Gao Lihao, Yan Zhongwei, Quan Xiaowei. 2015. Observed and SST-forced multidecadal variability in global land surface air temperature. Climate Dynamics, 44(1–2): 359–369, doi: 10.1007/s00382-014-2121-9

Gu Xiaoli, Li Peiliang. 2009. Pacific sea level variations and its factors. Haiyang Xuebao (in Chinese), 31(1): 28–36

Hamlington B D, Strassburg M W, Leben R R, et al. 2014. Uncovering an anthropogenic sea-level rise signal in the Pacific Ocean. Nature Climate Change, 4(9): 782–785, doi: 10.1038/NCLIMATE2307

Holgate S J, Matthews A, Woodworth P L, et al. 2013. New data systems and products at the permanent service for mean sea level. Journal of Coastal Research, 29(3): 493–504

Huang N E, Shen Zheng, Long S R, et al. 1998. The empirical mode decomposition and the Hilbert spectrum for nonlinear and non-stationary time series analysis. Proceedings of the Royal Society A: Mathematical, Physical and Engineering Sciences, 454 (1971): 903–995

Huang N E, Wu Zhaohua. 2008. A review on Hilbert-Huang transform: Method and its applications to geophysical studies. Reviews of Geophysics, 46(2): RG2006

Huang Zhenguo, Zhang Weiqiang, Wu Houshui, et al. 2001. A prediction of sea level rising amplitude in 2030 and defensive countermeasures in the Zhujiang Delta. Science in China Series D: Earth Sciences, 44(5): 446–454

IPCC. 2007a. Climate change 2007: Impacts, adaptation, and vulnerability. In: Parry M L, Canziani O F, Palutikof J P, et al., eds. Contribution of Working Group II to the Fourth Assessment Report of the Intergovernmental Panel on Climate Change. Cambridge: Cambridge University Press, 976

IPCC. 2007b. Climate change 2007: the physical science basis. In: Solomon S, Qin D, Manning M, et al., eds. Contribution of Working Group I to the Fourth Assessment Report of the Intergovernmental Panel on Climate Change. Cambridge: Cambridge University Press, 996

IPCC. 2013. Climate change 2013: the physical science basis. In: Stocker T F, Qin D, Plattner G K, et al., eds. Contribution of Working Group I to the Fifth Assessment Report of the Intergovernmental Panel on Climate Change. Cambridge: Cambridge University Press, 1535

Kharin V V, Zwiers F W, Zhang Xuebin, et al. 2007. Changes in temperature and precipitation extremes in the IPCC ensemble of global coupled model simulations. Journal of Climate, 20(8): 1419–1444

Li Juan, ZuoJuncheng, Chen Meixiang, et al. 2013. Assessing the global averaged sea-level budget from 2003 to 2010. Acta Oceanologica Sinica, 32(10): 16–23

Li Pingri, Fang Guoxiang, Huang Guangqing. 1993. Impacts of sea level rising on the economic development of Zhujiang Delta and countermeasures. Haiyang Xuebao (in Chinese), 48(6): 527–534

Li Xiang, Zhang Jianli, Gao Zhigang. 2011. Discussion on semi-empirical prediction method for sea level change of China. Marine Science Bulletin (in Chinese), 30(5): 540–543

Li You, Wang Yanglin, Peng Jian, et al. 2009. Assessment of loss of ecosystem service value under sea-level rise: A case study of Shekou Peninsula in Shenzhen. Progress in Geography (in Chinese), 28(3): 417–423

Liu Dujuan. 2004. Possible impacts of relative sea level rise in the coastal areas in China. Marine Forecasts (in Chinese), 21(2): 21–28

Massey F J Jr. 1951. The Kolmogorov-Smirnov test for goodness of fit. Journal of the American statistical Association, 46(253): 68–78

Moss R H, Edmonds J A, Hibbard K A, et al. 2010. The next generation of scenarios for climate change research and assessment. Nature, 463(7282): 747–756

NASA. 1998. The Development of the Joint NASA GSFC and the National Imagery and Mapping Agency (NIMA) Geopotential Model EGM 96. Washington: NASA, 584

Permanent Service for Mean Sea Level (PSMSL). 2014. Obtaining Tide Gauge Data http://www.psmsl.org/data/obtaining/[2014-6-6]

Qian Cheng, Zhou Tianjun. 2014. Multidecadal variability of North China aridity and its relationship to PDO during 1900–2010. Journal of Climate, 27(3): 1210–1222

Ren Meie, Zhang Renshun. 1993. Relative sea level changes in china over the last eighty years. Haiyang Xuebao (in Chinese), 15(5): 87–97

Shi Yafeng, Zhu Jiwen, XieZhiren, et al. 2000. Prediction and prevention of the impacts of sea level rise on the Yangtze River Delta and its adjacent areas. Science in China Series D: Earth Sciences, 43(4): 412–422

Sweet W, Zervas C, Gill S, et al. 2013. Hurricane sandy inundation probabilities today and tomorrow [in "Explaining extreme events of 2012 from a climate perspective"]. Bulletin of the American Meteorological Society, 94(9): S17–S20

Taylor K E, Stouffer R J, Meehl G A. 2012. An overview of CMIP5 and the experiment design. Bulletin of the American Meteorological Society, 93(4): 485–498

Wang Long. 2013. Study of sea level change and its influencing factor in the China sea based on nineteen year's altimeter data (in Chinese) [dissertation]. Qingdao: Ocean University of China, 1–63

Wang Hui, Liu Kexiu, Zhang Qi, et al. 2014. The relationship between sea level change of China's coast and ENSO. Haiyang Xuebao (in Chinese), 36(9): 65–74

Wu Tao, Kang Jiancheng, Li Weijiang, et al. 2007. Advance of sea level change research in China. Marine Geology & Quaternary Geology (in Chinese), 27(4): 123–130

Wu Zhaohua, Huang N E. 2009. Ensemble empirical mode decomposition: a noise-assisted data analysis method. Advances in Adaptive Data Analysis, 1(1): 1–41

Wu Zhaohua, Huang N E, Wallace J M, et al. 2011. On the time-varying trend in global-mean surface temperature. Climate Dynamics, 37(3–4): 759–773

Xia Jiangjiang, Yan Zhongwei, Wu Peili. 2013. Multidecadal variability in local growing season during 1901–2009. Climate Dynamics, 41(2): 295–305

Yim W W S. 1989. The impact of sea-water level. In: ProcInternational Conference on Atmosphere, Climate and Man, Torino, Italy

Zuo Juncheng, Yang Yiqiu, Zhang Jianli, et al. 2013. Prediction of China's submerged coastal areas by sea level rise due to climate change. Journal of Ocean University of China, 12(3): 327–334